International Journal of Rock Mechanics & Mining Sciences 87 (2016) 104–112

Contents lists available at ScienceDirect

International Journal of Rock Mechanics & Mining Sciences

journal homepage: www.elsevier.com/locate/ijrmms

Statistical analysis of the stability number adjustment factors and implications for underground mine design

J.A. Vallejos *, A. Delonca, J. Fuenzalida, L. Burgos

Department of Mining Engineering, Advanced Mining Technology Center, Faculty of Physical and Mathematical Sciences, University of Chile, Santiago, Chile

ARTICLE INFO

Article history:
Received 26 September 2015
Received in revised form
16 March 2016
Accepted 7 June 2016
Available online 20 June 2016

Keywords:
Mathews stability graph
Open stope design
Statistical evaluation
Stress factor
Deep underground mine

1. Introduction

The Mathews method[1] is widely used in underground hard rock mines in order to design open stopes and evaluate the stability of their geometry. The method consists in the construction of a stability graph that relates two calculated parameters: the shape factor, *S* and the stability number, *N*. The stability number *N* represents the ability of the rock mass to resist under a given stress condition. The shape factor *S*, or hydraulic radius, takes into account the size of the stope faces. The combination of these two parameters defines the stability of planned excavations. Four stability zones have been defined.[4] First, the *Stable Zone* represents the excavation which stand unsupported, or with localized support. Then, the *Failure Zone* represents the excavation where localized unravelling occurs, but a stable arch forms. Modifying the design or installing cable support may reduce the extent of the unravelling. The *Major Failure Zone* represents the cases where the extent of back or wall failure was greater than about fifty per cent of the smaller dimension of the opening. Finally, the *Caving zone* is defined. The cases falling in this zone indicate that the face of the stope under consideration is probably unsupportable and will fail and continue to fail until the void is completely filled or surface breakthrough occurs, i.e. a true caving situation.

The shape factor, *S*, and the stability number, *N*, are defined as follows:

$$S(m) = (\text{stope face area})/(\text{stope face perimeter}) \tag{1}$$

$$N = Q' \times A \times B \times C \tag{2}$$

where Q' is defined by[3]:

$$Q' = (RQD/J_n)(J_r/J_a) \tag{3}$$

and where *RQD* is the rock quality designation, J_n is the joint set number, J_r is the joint roughness number, and J_a is the joint alteration number. In Eq. (2), *A*, *B*, and *C* are respectively defined as the stress factor, the joint adjustment orientation factor, and the gravity factor. The rock stress factor, *A*, is a function of the ratio between the intact rock uniaxial compressive strength, σ_c, and the induced compressive stress, σ_1, estimated at the center of the stope face by

$$\text{ratio} = \sigma_c/\sigma_1 \tag{4}$$

The induced stress σ_1 can be found by numerical stress analysis or estimated from published stress distributions. The rock stress factor is determined from an empirical chart (Fig. 1a). The joint orientation adjustment factor, *B*, is a function of the relative difference in dip angle between the stope face and the critical joint set affecting stability (α), and is estimated using Fig. 1b. The gravity adjustment factor, *C*, reflects the stability of the orientation of the stope face under the influence of gravity, and it is determined from Eq. (5) or Fig. 1c.

* Correspondence to: Department of Mining Engineering, Advanced Mining Technology Center, Faculty of Physical and Mathematical Sciences, University of Chile, Chile.
E-mail address: javallej@ing.uchile.cl (J.A. Vallejos).

http://dx.doi.org/10.1016/j.ijrmms.2016.06.001
1365-1609/

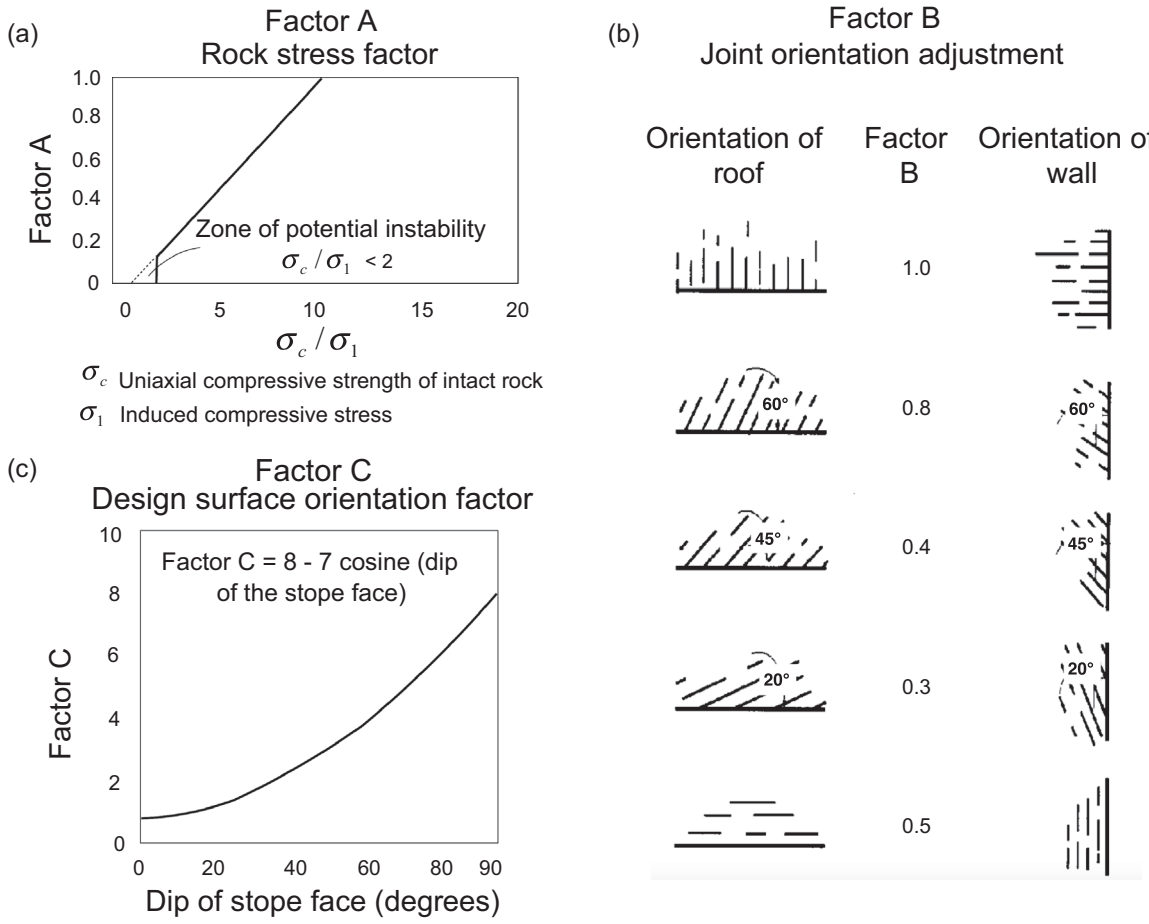

Fig. 1. Adjustment factors for determination of the Mathews stability number.[1]

$$C = 8\text{–}7\ \cos(\text{dip of stope face}) \quad (5)$$

As an empirical method, the stability graph presents some limitations. The most significant ones are[4]: the subjectivity in the definition of the stability zones, the absence of standardization of the extended database,[5] the non-representation of the rock stress factor, *A*, for instabilities caused by low confinement conditions, and the poor representation of the sliding failure modes by the gravity adjustment factor *C*. In the past three decades, several studies have addressed these limitations. Redefinition of the transition zones[2,6] and statistical analysis using a Bayesian likelihood statistic[7] have been proposed. The extension of the stability database[1] allowed to define statistically the Stable/Failure and Failure/Major-Failure boundaries using logistic regression.[8]

Modifications of the *A*, *B*, and *C* factors have also been proposed.[2,9–11] However, none of these studies have evaluated the impact of the proposed modifications on the performance of the method. Thus there is no evidence that the modifications are statistically significant.

Stewart and Trueman[12] investigated the goodness of the fit of logit models for different versions of the rock stress factor *A* for low stresses. Five rock stress factors were included in the analysis: the original Mathews stress factor, the Diederichs and Kaiser modified stress factor,[13] a reflected stress factor, Stewart's modified stress factor, and a fixed stress factor of 0.5.[5] This study concluded that the alternative stress factors did not improve the performance of the stability boundaries defined relative to the original stress factor.

Mawdesley et al.[18] used logistic regression to improve the definition of the stability boundaries. Three stability zones were defined: stable, failure and major failure. In a further study, Mawdesley[5] concluded that the failure – major failure boundary could not be correctly determined from the statistically analysis. Therefore, only the stable state from the other states of stability can be properly identified.

In this paper, statistical analysis is used to evaluate the performance and significance of the factors *A*, *B*, and *C* leading to the calculation of the stability number *N*. Based on a literature review and to the author's knowledge several adjustment factors are tested. The impact of these factors on the performance of the stable boundary is evaluated using a contingency matrix and a performance metrics analysis. The indicator of performance (Peirce Skill Score[14]) of the model, obtained for different combination of factors of adjustment, is maximized to define the most representative boundary of stability. The extended Mathews database[8] is considered as the reference for the analysis. The results lead to the proposal of a new rock stress factor that is less conservative than the original one for high stress conditions. The performance evaluation of different *B* and *C* factors did not improve the significance of the stability graph method compared to the original. The implications for underground mine design are evaluated and discussed in the last part of the paper.

2. Modifications to the stability number

The first modification of the stability graph method was proposed by Potvin[9] after collecting a significant amount of case histories for a range of mining depths (175 cases histories from 34 mines). The rock stress factor, *A*, is based on the proposal of

Mathews et al.[1] except for the case where the value of the ratio (intact rock strength/induced compressive stress) is lower than 2, where A becomes constant and equal to 0.1. The joint orientation adjustment factor, *B*, proposed by Potvin is also different from the one proposed by Mathews for angles between the stope face and the critical joint set between 0° and 45°. The gravity adjustment factor, *C*, was also modified by Potvin and is calculated by:

$$C = 8\text{–}6\ \cos(\text{dip of stope face}) \tag{6}$$

In addition, Potvin considered the failure mode in the analysis. The failure mode can be represented by the form of gravity fall, sliding or slabbing.

Recently, Bewick and Kaiser[10] proposed an adjustment to the joint orientation factor, *B*, based on two-dimensional continuum numerical modeling.

Mitri et al.[11] proposed an adjustment of the rock stress factor, *A*. They reported that the stability graph method is reliable in situations where the maximum induced tangential stress creates adequate compressive stress, keeping the face in a state of confinement. They thus proposed a new rock stress factor, which reflects the impact of low confinement on critical face stability.

The new rock stress factor, A', is determined by an asymptotic function as follows:

$$\text{For } MSF < 0.0,\ A' = 0.1 \tag{7}$$

$$\text{For } 0.0 \le MSF \le 1.0,\ A' = 0.1 + 0.9e\left[\left(-e^{-(\text{MSF}-0.3)/0.09} - (\text{MSF} - 0.3)/0.09 + 1\right)\right] \tag{8}$$

$$\text{For } MSF > 1.0,\ A' = 0.1 \tag{9}$$

where $MSF = 1/\text{ratio} = (\sigma_1/\sigma_c)$ is the maximum stress factor. Factor A' reaches a peak value of 1 when the value of *MSF* is 0.3 and decreases when the value of *MSF* is less than 0.1 or greater than 1.0.

3. Data and methods

3.1. Extended stability database

The extended stability database[5] is a combination of the original Mathews database and other cases reported elsewhere.[1,6,9,11,12,15] The extended stability database contains 465 case histories from over 38 mines in North America, Australia, Chile, and England (Table 1).

The extended database has been compiled from different mines around the world. Then, some subjectivity in the definition of the stability classes has to be recognized. However, the complete database is considered for this study as it represents the most representative collection of case histories to date.

3.2. The contingency matrix and performance metrics

The contingency matrix is used to test the performance of a classifier by comparing the prediction outcomes of the model to known values. For a two-class prediction problem, there are four possible situations.[16] If the actual value is positive and is classified as positive, it is counted as a true positive (*TP*); if it is classified as negative it is counted as a false negative (*FN*). If the actual value is negative and is classified as negative, it is counted as a true negative (*TN*); if it is classified as positive, it is counted as a false positive (*FP*). The information can be displayed in a two-by-two contingency matrix.

Based on the matrix, the following metrics are defined:

Table 1
Summary table of the number and stability condition of the case histories of the extended stability database. Stability of the stope face has been classified: S for Stable, F for Failure and MF for Major Failure. After Mawdesley.[5]

	Walls				Backs			
	S	F	MF	Total	S	F	MF	Total
Mathews et al.	2	2	–	**4**	4	9	2	**15**
Potvin	31	8	5	**44**	23	4	13	**40**
Nickson	4	2	3	**9**	2	–	2	**4**
Mount Charlotte	152	18	1	**171**	10	16	17	**43**
Cannington South Crofty	73	5	3	**81**	6	–	–	**6**
Complexe Bousquet	4	10	2	**16**	3	1	–	**4**
Newcastle	–	–	–	**–**	–	16	2	**18**
Caving Cases	–	–	–	**–**	–	–	11	**11**
Total (All)	266	45	14	**325**	48	46	47	**158**
	Total walls and backs				**314**	**91**	**61**	***465***

$$TPR = TP/(TP + FN);\ FPR = FP/(FP + TN);$$
$$ACC = (TP + TN)/(TP + FP + TN + FN) \tag{10}$$

The *True Positive Rate* (*TPR*) defines the percentage of positive cases that are correctly classified. Reversely, the *False Positive Rate* (*FPR*) defines the percentage of negative cases that are incorrectly classified. The *Accuracy* (*ACC*) defines the total percentage of correctly predicted outcomes. To measure the performance of the model, the *Peirce Skill Score* (*PSS*)[14] is used:

$$PSS = TPR\text{–}FPR \tag{11}$$

For a perfect classifier, $TPR = ACC = PSS = 1$ and $FPR = 0$. A PSS equal to zero corresponds to a random classifier.

3.3. Optimization procedure

To evaluate the performance of the adjustment factors, an optimization procedure has been developed based on the contingency matrix and performance metrics analysis. The stability boundaries are represented by the following general form[4,5]:

$$N = \beta^* S^{\gamma} \tag{12}$$

where *N* is the Mathews stability number, *S* is the shape factor, and γ and β are parameters obtained by optimization.

The proposed optimization procedure is defined by the following three steps. First, three scenarios of analysis are defined to distinguish the positive and negative values of the predicted outcome. The scenario 1 considers that the positive value correspond to the stable cases, while the negative value correspond to the failure+major failure cases. The scenario 2 considers the failure cases as positive value, and the stable+major failure cases as negative value. The scenario 3 considers the major failure cases as positive value, and the stable+failure cases as negative value. Next, for each scenario the *TPR*, *FPR*, and *PSS* are evaluated ((Eqs. (10) and 11)). Finally, in order to define a representative boundary, the γ and β parameters of Eq. (12) are changed until the *PSS* metric is maximized.

3.4. Considered adjustment factors for the analysis

3.4.1. Rock stress factor A

The following rock stress factors are considered for the performance evaluation of the stability boundaries (Fig. 2): (1) a factor *A* equal to 1 independent of the ratio σ_c/σ_1. This case assumes that there is no influence of the factor *A;* (2) the factor *A* proposed by Potvin[9]. This factor is considered as the original one in this study; (3) a modified version of the Stress Reduction factor (*SRF*)

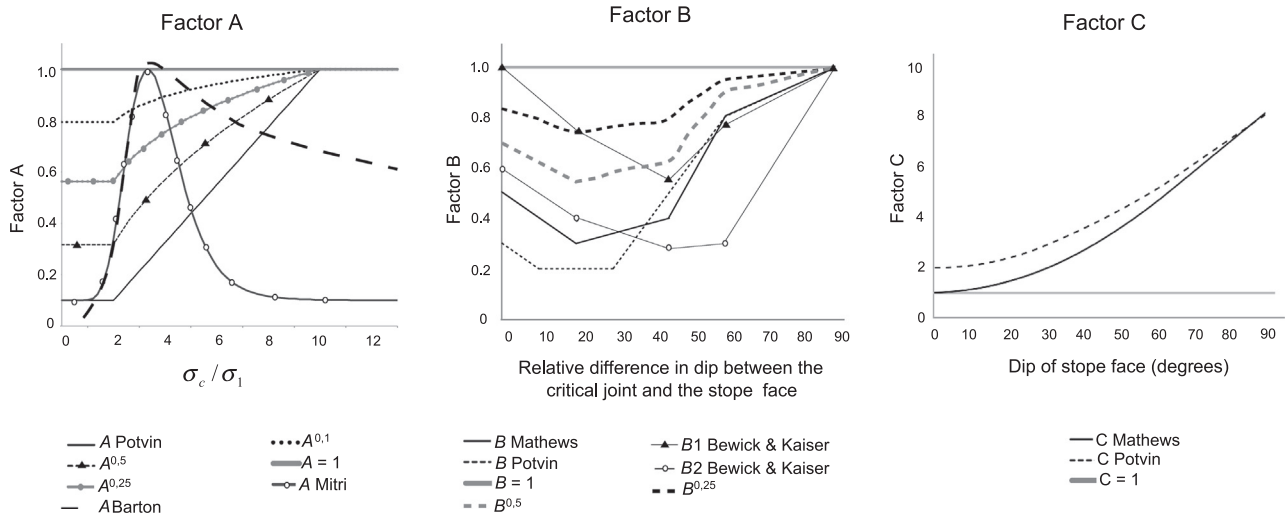

Fig. 2. Considered adjustment factors for the analysis and evaluation of performance of the stability boundaries.

proposed by Barton,[17] given by: $A=(1/(2\times SRF))$; (4) the factor A proposed by Mitri et al.[11] and (5) the original factor A raised to different exponents: $A^{0.1}$, $A^{0.25}$, $A^{0.5}$.

3.4.2. Joint orientation factor B

The following joint orientation factors are considered for the performance evaluation of the stability boundaries (Fig. 2): (1) a factor B equal to 1. This case assumes that there is no influence of joint orientation; (2) the factor B proposed by Mathews et al.[1] (Fig. 1b). This factor is considered as the original one in this study; (3) the factor B proposed by Potvin[9]; (4) the factors B proposed by Bewick and Kaiser[10] and (5) the original factor B raised to different exponents: $B^{0.25}$and $B^{0.5}$.

3.4.3. Gravity factor C

The following gravity factors are considered for the performance evaluation of the stability boundaries (Fig. 2): (1) a factor C equal to 1. This case assumes that there is no influence of the factor C; (2) the factor C proposed by Mathews et al.[1] (Fig. 1c). This factor is defined as the original one in this study and (3) the factor C proposed by Potvin.[9]

3.5. Combinations of adjustment factors

Different combinations of the adjustment factors are defined (Fig. 3). Firstly, the original adjustment factors are considered. The performance of the stability boundaries proposed by Mawdesley[8] are evaluated. In addition, the stability boundaries are determined by the optimization procedure proposed in this paper and

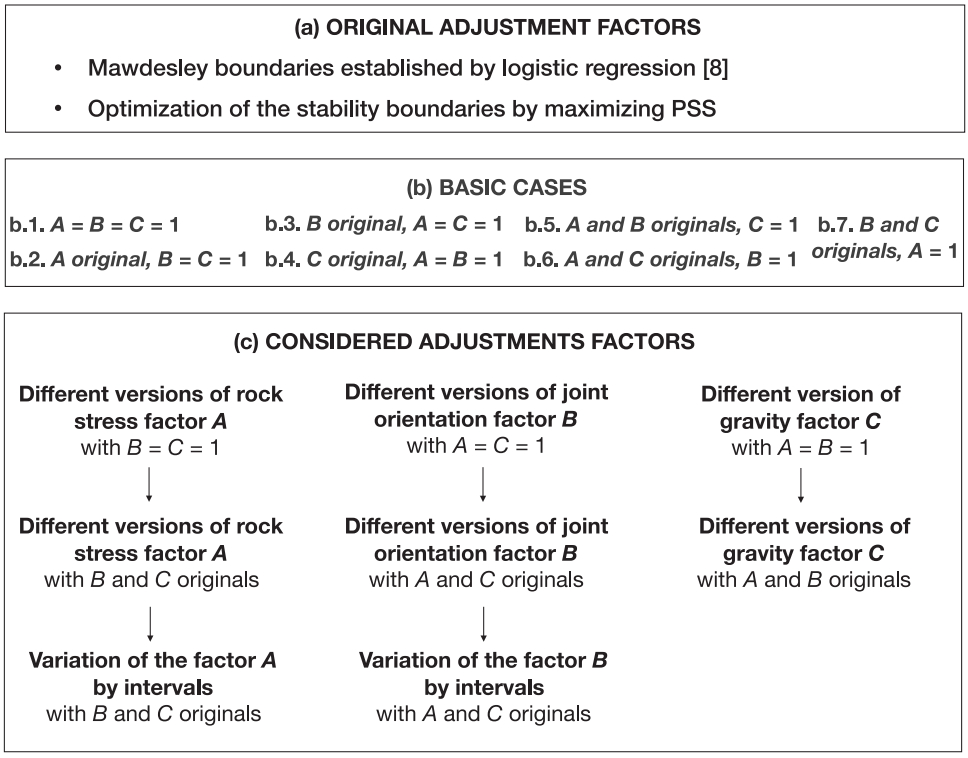

Fig. 3. Combinations of adjustment factors considered for the analysis and evaluation of performance of the stability boundaries.

compared to the ones obtained in[8] (Fig. 3a). Secondly, basic cases are defined to test the influence of combinations of the original adjustment factors by setting them individually or in groups to values equal to one (Fig. 3b). Thirdly, different combinations of the considered adjustment factors defined in Section 3.4 are evaluated (Fig. 3c).

3.6. Impact on stope design

To evaluate the influence of the adjustment factors on stope design, the maximum admissible shape factor S_{max} is defined. It represents the maximum shape factor for a face to be classified as stable and is defined by:

$$S_{max}=\sqrt[\gamma]{(Q'\times A\times B\times C)/\beta} \tag{13}$$

where Q' is the rock quality designation and A, B, and C are the adjustment factors. γ and β are the parameters of the boundary between the stable state and the other states of stability.

The admissible length per face L for both the back and the wall are defined by Eqs. (14) and (15), respectively. They represent the maximum length in which both faces are stable independently.

$$L_{back}=\frac{2wS_{max\ back}}{w-2S_{max\ back}} \tag{14}$$

$$L_{wall}=\frac{2hS_{max\ wall}}{w-2S_{max\ wall}} \tag{15}$$

where w is the width and h is the height of the stope, respectively. $S_{max\ back}$ and $S_{max\ wall}$ correspond to the maximum shape factor of the back and the wall, respectively.

In order to evaluate a relationship between the maximum admissible shape factor per face and the final geometry of the stope, the admissible length of the stope L_{stope} is defined. It represents the length in which both faces are stable simultaneously

$$L_{stope}=\min(L_{back}, L_{wall}) \tag{16}$$

Then, the admissible shape factor S for both faces is defined by the following equations:

$$S_{back}=\frac{wL_{stope}}{2(w+L_{stope})} \tag{17}$$

$$S_{wall}=\frac{hL_{stope}}{2(h+L_{stope})} \tag{18}$$

The variation of the admissible length of the stope, ΔL, and the shape factor evaluated for both faces, ΔS, are defined by

$$\Delta L=L_{original}-L_{considered} \tag{19}$$

$$\Delta S=S_{original}-S_{considered} \tag{20}$$

where $L_{original}$ and $S_{original}$ are the admissible length and shape factor obtained using the original adjustment factors. $L_{considered}$ and $S_{considered}$ corresponds to the admissible length and shape factor derived from the considered adjustment factors (Section 3.4).

The average percentage of variation of the admissible length, *PVL*, and the shape factor, *PVS*, are given by the following Equations.

$$\mathrm{PVL}=\frac{\sum_1^n(\Delta L/L_{original})}{n} \tag{21}$$

$$\mathrm{PVS}=\frac{\sum_1^n(\Delta S/S_{original})}{n} \tag{22}$$

where n is the number of cases in the database used to evaluate the performance of the considered adjustment factors.

4. Results

4.1. Original adjustment factors

Table 2 presents the parameters and associated performance metrics for the stability boundaries established in[18] and those determined by applying the proposed optimization procedure presented in Section 3.3. In accordance to Section 3.3 three scenarios are defined.

From Table 2 it can be concluded that the failure cases (scenario 2) in the database are not correctly identified (low *PSS*). In addition, the identification of stable cases (scenario 1) and major failure cases (scenario 3) have the higher *PSS*. The conclusion determined from the performance metrics analysis is similar to the one proposed by in[5]: the failure cases cannot be correctly identified. Note, that the *ACC* values for the three scenarios are high, which is not the case for the *PSS*. Therefore, the accuracy metric is limited for testing the randomness of the classifier, and it will not be included in the following analysis.

From Table 2 it can also be observed that the γ and β parameters of the boundary between the stable and the others cases determined using the developed optimization procedure are equal to those proposed in[18] using logistic regression. Fig. 4 presents the resulting stability boundaries.

4.2. Basic cases

Table 3 presents the determined parameters (γ and β) of the stable boundary and the associated performance metrics for the basic cases defined in Fig. 3a. The first exercise is to set all the factors equal to one. Next, two of the three factors are defined equal to one. Finally, only one of the factors is considered equal to one.

The results from Table 3 clearly indicate that the factor C is the most significant parameter (higher *PSS*) on the delimitation of the stable boundary. If the factor C is set equal to one, then factor A is more significant than the factor B. Finally, when only the A or B factors are set equal to one, the performance of the stability boundary does not change significantly.

4.3. Considered adjustment factors

4.3.1. Influence of factor A

In this section, the impact on the determined parameters (γ and β) of the stable boundary and the associated performance metrics for the different considered A factors is evaluated. First, the influence of the factor A is studied individually by considering the factors B and C equal to 1. The results are presented in Table 4a. It can be observed that for this case the original factor has the best performance metric. On the other hand, the A factor proposed by Mitri[11] has the lower *PSS*.

Table 4b presents the results by combining the different considered A factors with the original B and C factors. It can be observed that there is a small improvement of the *PSS* value when $A^{0.25}$ or $A^{0.5}$ are considered.

To further evaluate the influence of the factor A on the performance of the stable boundary, the ratio σ_c/σ_1 is divided into five intervals: (1) equal to or below 2, (2) between 2.01 and 4.22, (3) between 4.23 and 6, (4) between 6.01 and 10, and (5) higher

Table 2
Parameters γ and β, and associated performance metrics for; (a) the stability boundaries established by Mawdesley et al. [18] and (b) determined by applying the proposed optimization procedure. The higher values of *PSS* are highlighted in bold.

(a) Parameters					(b) Performance metrics				
	Boundary				Scenario				
	Mawlesdey et al.[18]		Proposed optimization procedure			Mawlesdey et al.[18]		Proposed optimization procedure	
	γ	β	γ	β		*PSS*	ACC	*PSS*	*ACC*
Stable/Failure	1.82	0.32	1.82	0.32	1	**0.64**	0.80	**0.64**	0.80
Failure/Major-Failure	1.82	0.07	1.76	0.26	2	0.27	0.75	0.06	0.79
					3	**0.65**	0.89	**0.65**	0.80

than 10. These intervals were selected in order to obtain equal number of cases for each interval. Note that for the first and last interval the *A* factor is constant and equal to 0.1 and 1, respectively.

Table 5 presents the performance metrics of the stable boundaries established in Table 4 divided by intervals. For the first interval, the best *PSS* is obtained for the factor $A^{0.5}$. For the second interval, there are two maximum: for the factors $A^{0.25}$ and $A^{0.5}$. For the third interval, the maximum value of *PSS* is reached for an *A* value equal to $A^{0.25}$. For the fourth interval, there are two maximum: for the factors $A^{0.1}$ and $A^{0.5}$. Finally, for the last interval, the best *PSS* is reached for the rock stress factor equal to $A^{0.1}$.

This analysis enables to identify local improvements in the definition of the A factor which are used to guide the definition of a new rock stress factor in Section 5.

4.3.2. *Influence of factor B*

The same analysis is realized considering the joint orientation factor *B*. First, the influence of the factor *B* is studied individually by considering the factors *A* and *C* equal to 1 (Table 6a). It can be observed that regardless the value of *B*, the *PSS* is low. Table 6b presents the results by considering the different *B* factors with the original *A* and *C* factors. Considering the original factor, the *PSS* is equal to 0.64. This value is obtained in five out of eight cases. This analysis does not lead to conclude that the joint orientation factors considered in the evaluation are better than the original one.

Table 6c presents the analysis by considering intervals to evaluate in more detail the influence of the factor *B*. The interval No. 1 considers values of α comprised between 20° and 50°. The interval No. 2 considers values of γ comprised between 0° and 20°, and 50° and 90°. The results show that there is no improvement in the *PSS* value compared to the initial one (*PSS*=0.64).

4.3.3. *Influence of factor C*

Finally, the influence of the factor *C* is studied. First the factors *A* and *B* are considered equal to 1 (Table 7a). Then, the original values of *A* and *B* are considered (Table 7b). The higher *PSS* is obtained using the original factor *C*. This analysis does not allow to evaluate the considered gravity factors better than the original one. Based on this result, no further analysis using intervals is performed.

Table 3
Determined parameters (γ and β) of the stable boundary and the associated performance metrics for the basic cases. The two higher values of *PSS* are highlighted in bold.

Basic cases		Stable boundary parameters		Metric
Case	Combination	γ	β	*PSS*
1	*A=B=C=1*	1.19	0.55	0.33
2	*A or.; B=C=1*	1.39	0.37	0.48
3	*B or.; A=C=1*	1.23	0.72	0.41
4	*C or.; A=B=1*	1.13	5.39	**0.64**
5	*A, B or.; C=1*	1.92	0.04	0.52
6	*B, C or.; A=1*	0.93	5.39	**0.64**
7	*A, C or.; B=1*	1.49	1.03	0.62

or.=original.

Table 4
Determined parameters (γ and β) of the stable boundary and the associated performance metrics for the different versions of *A*, considering: (a) *B=C=1* and (b) the original versions of *B* and *C*. The higher values of *PSS* are highlighted in bold.

Considered factor *A*	*(a) B=C=1*			*(b) Original versions of B and C*		
	γ	β	*PSS*	γ	β	*PSS*
Original	1.39	0.37	**0.48**	1.41	0.59	0.64
$A^{0.1}$	1.17	1.07	0.46	1.36	1.35	0.64
$A^{0.25}$	0.75	3.60	0.42	1.26	1.68	**0.67**
$A^{0.5}$	0.80	3.64	0.39	1.30	1.22	**0.67**
A Mitri	0.83	0.30	0.30	0.53	1.94	0.40
A SRF	0.76	1.62	0.39	1.35	0.90	0.62

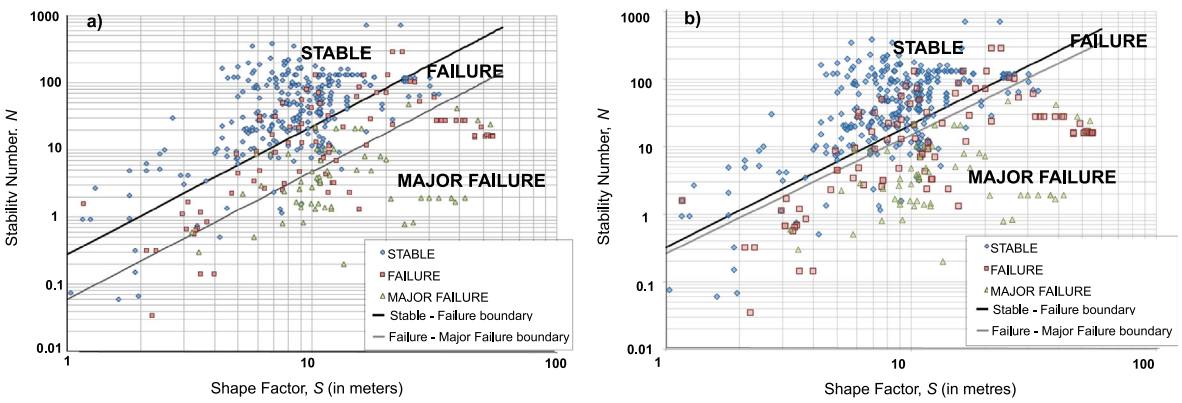

Fig. 4. Extended stability database on a log-log graph and the stability boundaries established by: (a) Mawlesdey et al.,[18] (b) applying the developed optimization procedure.

Table 5
Determined performance metrics of the stable boundary for different version of the considered *A* factors by dividing the data into intervals. Original values of *B* and *C* are considered. The higher values of *PSS* are highlighted in bold.

Interval	σ_c/σ_1	Data	*A or.*	$A=1$	$A^{0.5}$	$A^{0.25}$	$A^{0.1}$	*A* Mitri	A SRF
1	≤2	58	0.37	0.48	**0.56**	0.48	0.37	0.33	0.22
2	(2, 4.22)	83	0.68	0.76	**0.79**	**0.79**	0.73	0.40	0.63
3	(4.22, 6)	84	0.46	0.45	0.46	**0.49**	0.46	0.26	0.23
4	(6, 10)	85	0.64	0.70	**0.78**	0.75	**0.78**	0.47	0.41
5	≥10	155	0.55	0.61	0.60	0.63	**0.65**	0.10	0.47
Global PSS			0.64	0.64	0.67	0.67	0.64	0.40	0.62

or.=original.

Table 6
Determined parameters (γ and β) of the stable boundary and the associated performance metrics for different version of *B*, considering (a) $A=C=1$ and (b) the original values of *A* and *C*, and *(c)* two different intervals. The higher values of *PSS* are highlighted in bold.

Considered factor B	*(a) A=C=1*			*(b) Original values of A and C*			*(c) Intervals of γ*	
							No. 1 $20°<\alpha<50°$	No. 2 $0°\le\alpha\le20°$ & $50°\le\alpha\le90°$
	γ	β	*PSS*	γ	β	*PSS*	*PSS*	*PSS*
Original	1.22	1.01	0.41	1.41	0.59	**0.64**	**0.64**	**0.64**
Potvin	1.35	0.36	**0.43**	1.38	0.49	**0.64**	**0.64**	0.60
B1	1.55	0.31	0.39	1.35	1.21	0.63	0.62	0.60
B2	1.55	0.16	0.35	1.61	0.35	0.61	0.59	0.61
$B^{0.5}$	0.64	4.60	0.40	1.88	0.41	**0.64**	0.60	**0.64**
$B^{0.25}$	1.46	0.46	0.38	1.83	0.52	**0.64**	0.62	0.63

Table 7
Determined parameters (γ and β) of the stable boundary and the associated performance metrics for different version of *C*, considering (a) $A=B=1$ and (b) the original factors *A* and *B*. The higher values of *PSS* are highlighted in bold.

Considered factor C	*(a) A=B=1*			*(b) Original factors A and B*		
	γ	β	*PSS*	γ	β	*PSS*
Original	1.13	5.39	**0.64**	1.41	0.59	**0.64**
Potvin	1.34	3.58	0.61	1.54	0.76	0.63
C=1	1.19	0.55	0.33	1.45	0.65	0.63

5. Proposal of a new rock stress factor

Following the results of the analysis performed in Section 4.3.1, a new rock stress factor *A* is defined (Fig. 5). The implication from Fig. 5 is that when the values σ_c/σ_1 of are equal to or below 2, the value of *A* is equal to 0.32. This value is higher than the one considered by the original *A* factor. Moreover, when σ_c/σ_1 values are between 2 and 10, the new rock stress factor is higher than the original. Finally, when σ_c/σ_1 values are equal to or higher than 10, the value of the factor *A* is constant and equal to 1, resembling the original factor.

The performance of the new rock stress factor is tested using the optimization procedure. The results are presented in Table 8. The global *PSS* is equal to 0.68, which is marginally better than the best *PSS* value (0.67) of the considered adjustment factors of $A^{0.25}$ and $A^{0.5}$ (Table 4). However, the performance by interval of the stable boundary with the new rock stress factor has significantly improved.

Fig. 6 presents the boundaries of the stability zones established by Mawdesley et al.[18] using logistic regression and the boundary between the stable and the other cases using the new rock stress factor *A*. It can be observed that the new boundary has a lower slope in the log-log graph indicating that larger admissible shape factor can be obtained for some values of *N*. This will be addressed in more detail in Section 6.

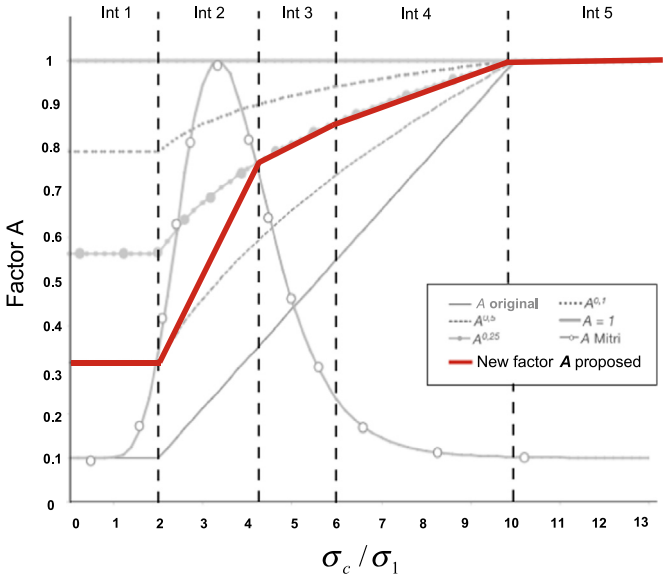

Fig. 5. Proposed new rock stress factor *A*.

Table 8
Determined parameters (γ and β) of the stable boundary and the associated performance metrics by interval for the original and proposed factor *A*.

Considered Factor *A*	γ	β	*PSS* for each σ_c/σ_1 interval					*Global*
			0.32	(0.32, 0.75)	(0.75, 0.85)	(0.85, 1)	1	*PSS*
Original factor	1.82	0.32	0.37	0.68	0.46	0.64	0.55	0.64
Proposed stress factor	1.48	0.46	0.56	0.79	0.49	0.78	0.65	0.68

6. Implications for underground mine design

In this section, the implications for underground mine design of using the proposed rock stress factor are evaluated. For this purpose 1000 synthetic cases of open stopes are defined. The transversal dimensions and the site conditions for each stope are considered to follow uniform probability distributions between an upper and lower limits (Table 9). K_h and K_v are the ratio of the horizontal and vertical stresses respectively.

The lower and upper values of Q' are established with respect to the limits presented in the extended Mathews stability database,[5] and range from 0.4 to 90. The values of the *B* factor are fixed and equal to 0.52 for the back and 0.53 for the wall. These values correspond to the average *B* values in the extended Mathews stability database.[5] The values of the *C* factor are equal to 1 for the back and 8 for the wall, based on the definition of the *C* factor.

For the evaluation, two different rock stress factor are considered: the original factor, *A*, and the proposed factor, $\bar{A}$. Firstly, the induced stresses per face are calculated using published curves.[1] Based on these stresses, the rock stress factor *A* and the stability number per face are calculated. The maximum admissible shape factor S_{max} (Eq. (13)), the admissible length per face *L* (Eqs. (14) and (15)) and the admissible length of the stope L_{stope} (Eq. (16)) are also calculated.

Finally, the average of the admissible shape factor *S* for both faces ((Eqs. (17) and 18)) is evaluated. Then, the average

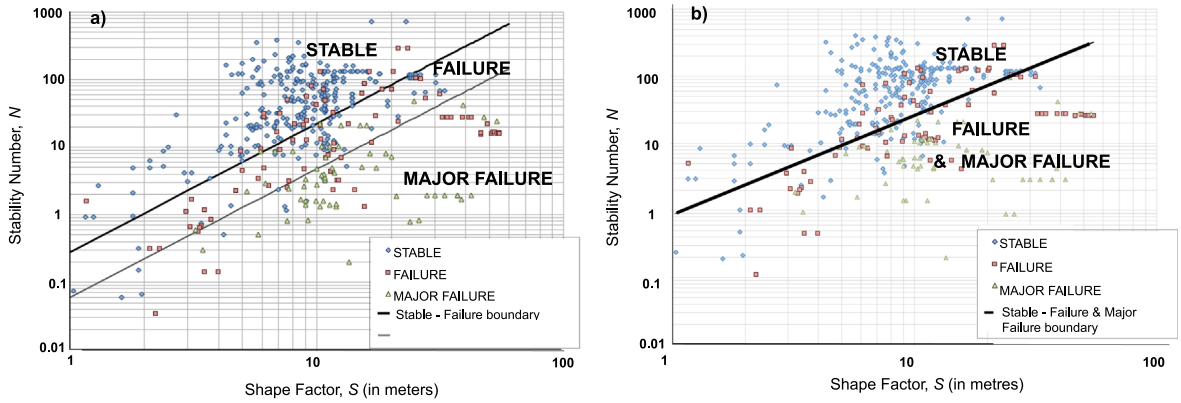

Fig. 6. Stability log-log graph presenting: (a) the boundaries of the stability zones established by Mawdesley et al.[18] using logistic regression and (b) the boundary between the stable and the other cases using the new rock stress factor *A*.

Table 9
Considered upper and lower limits for the transversal dimensions and site conditions for each stope.

	Width [m]	Height [m]	Depth [m]	K_v	K_h	*UCS* [MPa]
Lower limit	5	*Width*	500	0.5	0.5	50
Upper limit	30	8.*Width*	1000	2.0	2.0	150

percentage of variation of the admissible length, *PVL*, and the shape factor, *PVS* (Eqs. (21) and (22), respectively), as well as their associated standard deviation are evaluated (Table 9).

Table 10a shows that the average of the admissible stope length L_{stope} increase when the factor $\bar{A}$ is considered instead of the original one. It can be seen, that the average of the *PVL* highlights a difference of 84% in the admissible length between the original factor and the proposed one. This analysis demonstrates that the design of open stopes is remarkably impacted when considering the factor $\bar{A}$ and the new stability boundary. On average, the maximum length of the open stopes can be 84% larger.

Table 10b shows that both the averages of the admissible shape factor and the average percentage variation of the admissible shape factor *PVS* increase for each face when the factor $\bar{A}$ is considered. The *PVS* average highlights a difference between the original and the proposed factor *A* of 18% and 55% in the admissible *S* for the back and the wall, respectively.

7. Discussion and conclusions

The objective of the study presented in this paper is to evaluate the performance and significance of the adjustment factors used in the stability graph method. Several adjustment factors are considered, based on a literature review and to the authors knowledge. The performance of theses factors is evaluated using a contingency matrix and a performance metrics analysis. For each case of the considered adjustment factors, the performance metric is maximized to define the most representative boundary of stability.

The results and conclusions obtained using the proposed optimization procedure based directly on performance metrics analysis are similar to the ones reported in the literature using a logistic regression approach.[5,18]

Concerning the performance of the adjustment factors, the study highlights that there is no statistical evidence that the use of a modified factor of adjustment *B* or *C* is statistically significant. However, it seems that the factor *C* is the most significant parameter on the delimitation of the stable boundary. The use of a modified factor *A* is statistically significant, considering the original *B* and *C* factors. In particular, there is an improvement on the performance of the stable boundary model when the *A* factors are equal to $A^{0.25}$ or $A^{0.5}$.

Based on the statistical analysis performed in this study, a new rock stress factor *A* is proposed. The use of the proposed factor *A* leads to a modification of the stable boundary. This modification implies changes in the underground mine design. It leads to an

Table 10
Average of (a) admissible stope length and *PVL* and (b) admissible *shape factor* and *PVS* for the original and proposed rock stress factors and considering 1000 synthetic cases of open stopes.

(a) Admissible length of stope

Factor	*PSS*	γ	β	*Average of admissible length (m)*	*Sd of admissible length (m)*	*Average of PVL%*	*Sd of PVL%*
A	0.64	1.82	0.32	61.8	46.5	–	–
$\bar{A}$	0.68	1.48	0.46	103.5	52.5	**−83.7%**	**−85.2%**

(b) Admissible shape factor per face of the stope

Factor	*PSS*	γ	β	*Average of admissible shape factor (m)*		*Sd of admissible shape factor (m)*		*Average of PVS %*		*Sd of PVS%*	
				Back	*Wall*	*Back*	*Wall*	*Back*	*Wall*	*Back*	*Wall*
A	0.64	1.82	0.32	5.03	12.08	2.49	7.45	–	–	–	–
$\bar{A}$	0.68	1.48	0.46	5.88	17.04	2.93	10.09	**−18.0%**	**−54.8%**	**−22.9%**	**−45.7%**

PSV=percentage variation of admissible values of *S*. *Sd*=*Standard deviation*
A: original factor A. $\bar{A}$: proposed factor A.

increase of the admissible length and the admissible shape factor, resulting in a significant increase in the size of the open stope. Thus, the proposed factor *A* improves the predictive capabilities of the stability graph method.

In despite of these results, the reader has to note that the stability graph method and the proposed rock stress factor *A* do not consider rockbursting conditions. At depth, the risk for rockbursting and major seismic events increases and thus typically becomes the criteria for stope sizing and not the stability graph method. Therefore the proposed rock stress factor has to be used with caution when dealing with deep underground mines.

It has to be accepted that the empirical data is subjected to subjectivity and non-accurate measurements. However, several statistical analysis of the stability database have been performed[5,6,8,9,12,15,18] as summarized in.[4] All of these statistically analysis have improved the predictive capabilities of the approach and have directed to a better understanding and development of the design approach.

To improve the definition of the adjustment factors and the predictive capabilities of the stability graph method, it is recommended to develop a standardized database. A standardized database is defined here as a combination of cases histories from multiple sources that has been collected, processed and analyzed with a standardized procedure. Moreover, the sustainable growth of mining requires a review and standardization of the design methods. With this objective, an integrated technological platform MineRoc®[19] is under development. MineRoc includes an acquisition platform for mine data and geotechnical information, a geomechanical design module for stopes, and a back-analysis platform for calibrating mine design tools. The application and benefits of MineRoc have been illustrated for sublevel open stope Chilean mining operations.

Acknowledgments

The authors would like to acknowledge the financial support of the Chilean Government through the Project CORFO 11IDL2-10630 entitled “Development of Design Tools for Selective Underground Mining in Chile”, carried out at the Department of Mining Engineering and at the Advanced Mining Technology Center (AMTC) of the University of Chile.

References

1. Mathews KE, Hoek E, Wyllie DC, Steward SBV. *Prediction of Stable Excavations for Mining at Depths Below 1000 m in Hard Rock. CANMET Report DSS Serial no. OSQ80–00081, DSS File no. 17SQ.23440-0-9020.* Ottawa: Dept Energy, Mines & Resources; 1981.
2. Stewart SBV, Forsyth WW. The Mathew's method for open stope design. *CIM Bull.* 1995;88:45–53.
3. Barton N, Lien R, Lunde J. Engineering classification of rock masses for the design of tunnel support. *Int J Rock Mech Min Sci.* 1974;6:189–236.
4. Suorineni FT. The stability graph after three decades in use: experiences and the way forward. *Int J Min Reclam Environ.* 2010;24:307–339.
5. Mawdesley CA. *Predicting Rock Mass Cavability in Block Caving Mines [Ph.D. thesis].* Australia, Brisbane: University of Queensland; 2002.
6. Nickson SD. *Cable Support Guidelines for Underground Hard Rock Mine Operations [MSc. thesis].* Vancouver: Univ British Columbia; 1992.
7. Suorineni FT. *Effects of Faults and Stress on Open Stope Design [Ph.D. thesis].* Waterloo: University Of Waterloo, Canada; 1998.
8. Mawdesley CA. Using logistic regression to investigate and improve an empirical design method. *Int J Rock Mech Min Sci.* 2004;41:756–761.
9. Potvin Y. *Empirical Open Stope Design in Canada [Ph.D. thesis].* Vancouver: Dept Mining & Mineral Processing, Univ British Columbia; 1988.
10. Bewick RP, Kaiser PK. Numerical assessment of factor B in Mathews' method for open stope design. In: *Proceedings of the 3rd CANUS Rock Mechanics Symposium*. Toronto; 11–13 May 2009.
11. Mitri HS, Hughes R, Zhang Y. New rock stress factor for the stability graph method. *Int J Rock Mech Min Sci.* 2011;48:141–145.
12. Stewart PC, Trueman R. The extended mathews stability graph: quantifying case history requirements and site-specific effects. In: *Proceedings of International Symposium on Mining Techniques*, Chicago: CIM; 2001, 84–92.
13. Diederichs MS, Kaiser PK. Rock instability and risk analyses in open stope mine design. *Can Geotech J.* 1996;33:431–439.
14. Peirce CS. The numerical measure of the success of predictions. *Science.* 1884;4:453–454.
15. Trueman R, Mikula P, Mawdesley CA, Harries N. Experience in Australia with the application of the Mathews' method for open stope design. *CIM Bull.* 2000;93:162–167.
16. Fawcett T. An introduction to ROC analysis. *Pattern Recognit Lett.* 2006;27:861–874.
17. Barton N. Some new Q-value correlations to assist in site characterisation and tunnel design. *Int J Rock Mech Min Sci.* 2002;39:185–216.
18. Mawdesley CA, Trueman R, Whiten WJ. Extending the Mathews stability graph for open–stope design. *Min Technol.* 2001;110:27–39.
19. Vallejos JA, Miranda O, Gary C, Delonca A. Development of an integrated platform for stability analysis and design in sublevel stoping mines – MineRoc©. In: *Underground Design Methods 2015*. Perth. 17–19 November 2015: 477–489.